KELDYSH INSTITUTE OF APPLIED MATHEMATICS RUSSIAN ACADEMY OF SCIENCES

A.I.Neishtadt, D.J.Scheeres, V.V.Sidorenko, P.Stooke, A.A.Vasiliev

REACTIVE TORQUE INFLUENCE ONTO ROTATION OF COMET NUCLEI

 $\mathop{\rm MOSCOW}_{2002}$

A.I.Neishtadt, D.J.Scheeres, V.V.Sidorenko, P.Stooke, A.A.Vasiliev.

Reactive torque influence onto rotation of comet nuclei

Reactive torques, due to anisotropic sublimation on a comet nucleus surface, produce slow variations of its rotation. In this paper the secular effects of this sublimation are studied. The general rotational equations of motion are averaged over unperturbed fast rotation around the mass center (Euler-Poinsot motion) and over the orbital comet motion. We discuss the parameters that define typical properties of the rotational evolution and discover different classifications of the rotational evolution. As an example we discuss some possible scenarios of rotational evolution for the nuclei of the comets Halley and Borrelly.

А.И.Нейштадт, Д.Дж.Шиерс, В.В.Сидоренко, Ф.Стук, А.А.Васильев.

Влияние реактивных моментов на вращение кометных ядер

Реактивные моменты, возникающие при анизотропной сублимации вещества с поверхности кометного ядра, приводят к постепенному изменению его вращательного движения. Данная работа посвящена исследованию возможных вековых эффектов. Уравнения, описывающие вращение ядра, усредняются по невозмущенному движению ядра относительно центра масс (по движению Эйлера-Пуансо) и по орбитальному движению. Указаны параметры, определяющие характерные особенности эволюции вращения; дана классификация различных типов эволюции. В качестве примера обсуждаются возможные варианты эволюции вращения ядер комет Галлея и Борелли.

1.Statement of the problem and main assumptions

In the classical model of a comet nucleus suggested by F. Whipple [26], anisotropic ice sublimation due to solar radiation produces reactive torques, \mathbf{M}^r , that act on the nucleus. The goal of the present paper is to study the possible secular effects produced by \mathbf{M}^r on the rotational dynamics of the nucleus. Unlike previous studies, based primarily on numerical modeling of nucleus rotation evolution [9, 10, 20, 21, 24, 27], we use an averaging method [1, 5] to extract the secular components of the nucleus motion.

We approximate the nucleus surface by a polyhedron with an arbitrary number of faces. As an example, Fig. 1 shows such an approximation for the comet Halley nucleus. The shape of this nucleus is reconstructed on the basis of TV images obtained by missions "Vega-1,2" and "Giotto" [22, 23].

Reactive torques due to ice sublimation can be evaluated with the use of the approximate formula:

$$\mathbf{M}^r = -\sum_{j=1}^N Q_j(\mathbf{R}_j \times \mathbf{v}_j), \tag{1}$$

where N is the number of faces of the approximating polyhedron, Q_j is the mass ejection rate on the j-th face, \mathbf{R}_j is the radius vector of the face's center in the body principal frame of reference, and \mathbf{v}_j is the effective velocity of the ejected matter.

The mass ejection rate depends on local illumination conditions and the heliocentric distance, and is difficult to describe accurately [6]. Following [20, 10, 21], to calculate Q_j in this paper we use an empirical expression

$$Q_j = s_j g(r) f(\delta_j) Q_* \,. \tag{2}$$

Here Q_* is the mass ejection rate from a plane surface of area equal to the total surface area of the nucleus, oriented perpendicular to the Sun line of sight at a heliocentric distance of 1 AU, s_j is the relative intensity (the ratio of the maximal possible mass ejection rate from the j-th face at this heliocentric distance to Q_*), δ_j is the angle between the outer normal to the face \mathbf{n}_j and the unit vector pointing to the Sun \mathbf{e}_s , and r is the heliocentric distance.

The function g(r) describes the dependence of the mass ejection rate on the heliocentric distance. It is given by the expression [17]:

$$g(r) = g_0 \left(\frac{r}{r_0}\right)^{-c_1} \left[1 + \left(\frac{r}{r_0}\right)^{c_2}\right]^{-c_3}, \tag{3}$$

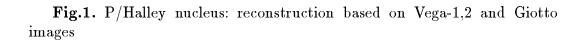


Fig.2. Angles and coordinate systems used to describe the comet nucleus motion

where

$$c_1 = 2.15, c_2 = 5.093, c_3 = 4.6142, r_0 = 2.808, g_0 = 0.111262.$$

The function $f(\delta_j)$ defines the dependence of the mass ejection rate on the angle between the direction to the Sun and the normal to the j-th face. Following [25], we assume that

$$f(\delta_i) = 1 - \alpha(1 - \cos \delta_i). \tag{4}$$

The coefficient α in Eq.(4) can be chosen to be 1/2 or slightly less.

We consider reactive torques as the only factor changing the nucleus rotation state; thus, we neglect variations in the nucleus shape and its moments of inertia due to matter sublimation. In addition, we neglect energy dissipation due to non-stationary deformations of the rotating nucleus caused by inertia forces. This approach is quite traditional in studies of spin evolution of short-period comets on time periods several tens or hundred orbits around the Sun [21]. We also assume that the comet orbit, defined by eccentricity e and perihelion distance q, does not change (in the future we plan to study the influence of the orbit evolution on the evolution of the rotational state).

2. Equations of motion

To describe the rotation of the comet nucleus, we introduce three right-hand orthogonal coordinate systems with their origin at the center of mass of the nucleus (Fig. 2):

OXYZ: The "perihelion" system, with the OZ-axis parallel to the Sunperihelion line, the OY-axis normal to the plane of the orbit, and the OX-axis parallel to the tangent to the orbit at perihelion and directed along the orbit motion;

Oxyz: The frame connected with the angular momentum vector of the nucleus **L**. The Oz axis is directed along **L**, the Oy axis is in the plane OXY;

 $O\xi\eta\zeta$: the body-fixed system, the axes $O\xi$, $O\eta$, $O\zeta$ being the principal inertia axes. The moments of inertia of the nucleus with respect to these axes are defined as A_*, B_*, C_* respectively, and satisfy the condition

$$A_* > B_* > C_*$$
.

We define the orientation of the coordinate system Oxyz with respect to the "perihelion" system OXYZ with the use of the angles ρ and σ (Fig. 2). A turn through the angle σ around the OZ axis followed by a turn through the angle ρ around the Oy axis puts the trihedron Oxyz into its current position from

an initial position coinciding with the trihedron OXYZ. The corresponding transfer matrix has the form:

We define the orientation of the system $O\xi\eta\zeta$ with respect to the system Oxyz by the Euler angles φ, ϑ, ψ . The transfer matrix is

The complete set of equations of the comet nucleus motion consists of the equations describing its rotation in the coordinate system Oxyz and the equations for the time evolution of its angular momentum vector.

It is convenient to use dimensionless variables and parameters in the equations of motion. Take as an independent variable $\tau = \Omega_* t$, where Ω_* is the initial angular velocity of the nucleus. The dimensionless variable L is the ratio of the magnitude of the angular momentum vector to $L_* = I_* \Omega_*$ (here $I_* = m_* R_*^2$, m_* is the nucleus mass, and R_* is its typical linear size). Then the parameters A, B, C are the dimensionless moments of inertia:

$$A = \frac{A_*}{I_*}, \ B = \frac{B_*}{I_*}, \ C = \frac{C_*}{I_*}.$$

For example, if the nucleus shown in Fig. 1 is homogeneous and $R_* = 5$ km is taken as its typical linear size, we have

$$A = 0.6121, \ B = 0.5857, \ C = 0.2129.$$

Relations for moments of inertia of celestial bodies of irregular shape approximated by polyhedrons are given in [7].

Taking into account the assumptions made above, we can write the equations of motion in the following form [3]:

$$\frac{d\vartheta}{d\tau} = L\sin\vartheta\sin\psi\cos\psi\left(\frac{1}{A} - \frac{1}{B}\right) + \\
+ \frac{1}{L}\left[\left(M_{\xi}^{r}\sin\psi + M_{\eta}^{r}\cos\psi\right)\cos\vartheta - M_{\zeta}^{r}\sin\vartheta\right], \\
\frac{d\varphi}{d\tau} = L\left(\frac{\sin^{2}\psi}{A} + \frac{\cos^{2}\psi}{B}\right) - \frac{M_{x}^{r}}{L}\cos\varphi\cot\vartheta - \\
- \frac{M_{y}^{r}}{L}(\cot\varphi + \sin\varphi\cot\vartheta), \\
\frac{d\psi}{d\tau} = L\cos\vartheta\left(\frac{1}{C} - \frac{\sin^{2}\psi}{A} - \frac{\cos^{2}\psi}{B}\right) + \frac{M_{\xi}^{r}\cos\psi - M_{\eta}^{r}\sin\psi}{L\sin\vartheta}, \\
\frac{d\rho}{d\tau} = \frac{M_{x}^{r}}{L}, \quad \frac{d\sigma}{d\tau} = \frac{M_{y}^{r}}{L\sin\varphi}, \quad \frac{dL}{d\tau} = M_{z}^{r}.$$
(5)

The values M_x^r, M_y^r, M_z^r and $M_{\xi}^r, M_{\eta}^r, M_{\zeta}^r$ in equations (5) are the projections of the reactive torque onto the corresponding axes of the coordinate systems Oxyz and $O\xi\eta\zeta$:

$$M_x^r = a_{x\xi} M_\xi^r + a_{x\eta} M_\eta^r + a_{x\zeta} M_\zeta^r,$$

and similarly for M_y^r and M_z^r with

$$M_{\xi}^{r} = \varepsilon g(r) \sum_{j=1}^{N} s_{j} d_{j\xi} [(1 - \alpha) + \alpha(\mathbf{e}_{s}, \mathbf{n}_{j})],$$

and similarly for M_{η}^{r} and M_{ζ}^{r} , where

$$\left(egin{array}{c} d_{j arepsilon} \ d_{j \eta} \ d_{j \zeta} \end{array}
ight) = \mathbf{n}_{j} imes \left(rac{\mathbf{R}_{j}}{R_{st}}
ight), \; arepsilon = rac{v_{st} Q_{st} R_{st}}{I_{st} \Omega_{st}^{2}}.$$

Here v_* is the effective velocity of ejected matter.

The parameter ε determines the influence of the reactive torque on the nucleus rotation. Considering ε as a small parameter (in this case the motion is a weakly perturbed Euler-Poinsot motion), we use the averaging method to develop a qualitative description of the solutions of (5). The adequacy of the assumption $\varepsilon \ll 1$ is confirmed for several short-period comets (see Table 1).

Table I. Typical parameter values derived from published data [9, 11]

$\overline{\text{Comet}}$	Q_*	R_*	$m_* \cdot 10^{-12}$	$I_* \cdot 10^{-12}$	Ω_*	arepsilon
\mathbf{name}	$[\mathrm{kg}\ \mathrm{h}^{-1}]$	[km]	[kg]	$[\mathrm{kg} \; \mathrm{km}^2]$	$[\mathrm{hr}^{-1}]$	
	J	upiter	family co	mets		
$2\mathrm{P/Encke}$	$5.1 \cdot 10^7$	2.3	53.7	294	0.97	$3.9\cdot 10^{-4}$
46P/Wirtanen	$3.4\cdot 10^6$	0.6	0.9	0.32	1	$5.7\cdot 10^{-3}$
$9\mathrm{P/Tempel}\ 1$	$5.1\cdot 10^7$	2.3	53.7	380	0.15	$1.2 \cdot 10^{-2}$
19P/Borrelly	$1.5\cdot 10^8$	4	85	1360	0.25	$6.4 \cdot 10^{-3}$
Halley-like comets						
$1\mathrm{P/Halley}$	$2.3\cdot 10^8$	5	525	13100	0.1	$7.9\cdot 10^{-3}$
109P/Swift- Tuttle	$1.3\cdot 10^9$	12	7240	10^{6}	0.1	$1.4 \cdot 10^{-3}$

Note an important property of the system (5): if

$$(\vartheta(\tau), \rho(\tau), \sigma(\tau), L(\tau), \psi(\tau), \varphi(\tau))$$

is its solution, then

$$(\pi - \vartheta(-\tau), \pi - \rho(-\tau), \pi + \sigma(-\tau), L(-\tau), \pi + \psi(-\tau), \pi - \varphi(-\tau))$$

is also its solution. This "reversibility" of solutions is due to absence of dissipation in the model of forces determining the comet nucleus dynamics.

3. Averaging approximation

3.1.Unperturbed motion

To successfully apply the averaging method and interpret the results one should take into consideration the following properties of the unperturbed motion.

At $\varepsilon = 0$ equations (5) describe the Euler-Poinsot case of a rigid body motion. In that case variables L, σ, ρ are independent of τ and the behavior of variables φ, ϑ, ψ can be described in terms of the Jacobi elliptic functions [15]. The nucleus' inertia ellipsoid rolls without slipping on a fixed plane Π perpendicular to the constant vector of angular momentum \mathbf{L} . Points of the inertia ellipsoid that are tangent to the plane Π at different times form a closed curve (polhode). Depending on initial conditions, this curve encircles either $O\xi$ or $O\zeta$ axis (Fig. 3).

Fig.3. The inertia ellipsoid and polhodes

One can use the following first integral of system (5) for $\varepsilon = 0$ to define the polhode on the inertia ellipsoid:

$$w = rac{2BT}{L^2} = \left[1 - \left(1 - rac{1}{ heta_A}\right)\sin^2\psi\right]\sin^2\vartheta + rac{\cos^2\vartheta}{ heta_C},$$
 $heta_A = rac{A}{B}, \; heta_C = rac{C}{B}.$

where

If $w \in \left(\frac{1}{\theta_A}, 1\right)$, the motion is called a complex short axis mode (complex SAM): the polhodes encircle the shortest axis of the inertia ellipsoid $O\xi$. If $w \in \left(1, \frac{1}{\theta_C}\right)$, the motion is called a complex long axis mode (complex LAM): the polhodes encircle the longest axis of the inertia ellipsoid $O\zeta$. At $w = \frac{1}{\theta_A}$ the polhodes degenerate into points, corresponding to rotation around the axis with the largest inertia momentum (simple SAM). Similarly $w = \frac{1}{\theta_C}$ corresponds to rotation around the axis with the smallest inertia momentum (simple LAM). Note, these classifications of motion are not usual and cannot be found in classic monographs on rigid body dynamics. Nevertheless, they are often used in studies of the rotation of celestial bodies (see, for example, [13, 21]).

If w=1, the motion is asymptotic: as $\tau \to \pm \infty$ the immediate rotation axis tends to the $O\eta$ axis. The polhodes corresponding to the asymptotic motions are separatrices separating polhodes of complex SAM and complex LAM (Fig. 3).

SAMs (complex and simple) can be divided into subsets SAM₊ and SAM₋ where the projection of the angular velocity vector $\boldsymbol{\omega}$ onto the axis $O\xi$ is correspondingly positive or negative. In the same way LAMs are divided into subsets LAM₊ and LAM₋ with different signs of projection of $\boldsymbol{\omega}$ onto $O\zeta$ axis.

3.2. Construction of evolutionary equations

The evolutionary equations are the closed set of equations for the secular components of variation in the variables σ, ρ, L and the value of w, which varies at $\varepsilon \neq 0$ in accordance with

$$\begin{split} \frac{dw}{d\tau} &= \frac{2(\boldsymbol{\omega}\,,\mathbf{M}^r)}{L^2} - \frac{2w}{L}\frac{dL}{d\tau} = \\ &= \frac{2}{L}\left[\left(\frac{1}{\theta_A} - w\right)a_{z\xi}M_\xi^r + (1-w)a_{z\eta}M_\eta^r + \left(\frac{1}{\theta_C} - w\right)a_{z\zeta}M_\zeta^r\right]\,. \end{split}$$

In the following w is used as a variable for describing motion of the nucleus with respect to the angular momentum vector.

We construct the evolutionary equations in two steps. First, the right hand sides of the equations for $\frac{dw}{d\tau}$, $\frac{d\sigma}{d\tau}$, $\frac{d\rho}{d\tau}$, $\frac{dL}{d\tau}$ are averaged along the unperturbed motion (Euler-Poinsot motion). SAMs and LAMs are described by different formulae and thus need to be considered separately (however, after a change of notation the expressions for SAMs and LAMs are similar). The second step is to average the equations over the orbital motion.

3.3. Evolutionary equations in the first approximation of the averaging method

Omitting tedious calculations, we present the evolutionary equations obtained:

$$\frac{dw}{d\tau} = \frac{2\varepsilon}{L} \left\{ (1-\alpha)\Phi_0 \left[D_0^{\xi} \langle a_{z\xi} \rangle_e \left(\frac{1}{\theta_A} - w \right) + D_0^{\zeta} \langle a_{z\zeta} \rangle_e \left(\frac{1}{\theta_C} - w \right) \right] - (6) \right.$$

$$-\alpha \cos \rho \Phi_1 \left[D_1^{\xi} \left(\left(\frac{1}{\theta_A} - w \right) \langle a_{z\xi}^2 \rangle_e - (1-w) \langle a_{z\eta}^2 \rangle_e \right) + \right.$$

$$+ D_1^{\zeta} \left(\left(\frac{1}{\theta_C} - w \right) \langle a_{z\zeta}^2 \rangle_e - (1-w) \langle a_{z\eta}^2 \rangle_e \right) \right] \right\},$$

$$\frac{d\rho}{d\tau} = -\frac{\varepsilon \alpha \sin \rho \Phi_1}{2L} \left[D_1^{\xi} (\langle a_{z\xi}^2 \rangle_e - \langle a_{z\eta}^2 \rangle_e) + D_1^{\zeta} (\langle a_{z\zeta}^2 \rangle_e - \langle a_{z\eta}^2 \rangle_e) \right],$$

$$\frac{d\sigma}{d\tau} = \frac{\varepsilon \alpha \Phi_1}{2L} \left(D_2^{\xi} \langle a_{z\xi} \rangle_e + D_2^{\zeta} \langle a_{z\zeta} \rangle_e \right),$$

$$\frac{dL}{d\tau} = \varepsilon \left\{ (1-\alpha)\Phi_0 \left(D_0^{\xi} \langle a_{z\xi} \rangle_e + D_0^{\zeta} \langle a_{z\zeta} \rangle_e \right) -$$

$$-\alpha \cos \rho \Phi_1 \left[D_1^{\xi} (\langle a_{z\xi}^2 \rangle_e - \langle a_{z\eta}^2 \rangle_e) + D_1^{\zeta} (\langle a_{z\zeta}^2 \rangle_e - \langle a_{z\eta}^2 \rangle_e) \right] \right\}.$$

For the secular components in (6) we use a notation that coincides with the corresponding variables; $\langle a \rangle_e$ is the average of $a(\varphi(\tau), \vartheta(\tau), \psi(\tau))$ in the Euler-Poinsot motion,

$$D_0^{\xi} = \sum_{j=1}^{N} s_j d_{j\xi}, \ D_1^{\xi} = \sum_{j=1}^{N} s_j d_{j\xi} n_{j\xi}, \ D_2^{\xi} = \sum_{j=1}^{N} s_j (d_{j\zeta} n_{j\eta} - d_{j\eta} n_{j\zeta}),$$

$$D_0^{\zeta} = \sum_{j=1}^{N} s_j d_{j\zeta}, \ D_1^{\zeta} = \sum_{j=1}^{N} s_j d_{j\zeta} n_{j\zeta}, \ D_2^{\zeta} = \sum_{j=1}^{N} s_j (d_{j\eta} n_{j\xi} - d_{j\xi} n_{j\eta}),$$

$$\Phi_0 = \frac{(1 - e^2)^{3/2}}{\pi} \int_0^{\pi} \frac{g(r(\nu)) d\nu}{(1 + e \cos \nu)^2},$$

$$\Phi_1 = \frac{(1 - e^2)^{3/2}}{\pi} \int_0^{\pi} \frac{\cos \nu g(r(\nu)) d\nu}{(1 + e \cos \nu)^2}.$$

In the last two formulae we integrate over the true anomaly ν .

If $\frac{1}{\theta_A} \leq w < 1$ (SAM motion), then

$$\langle a_{z\xi} \rangle_e = \pm \sqrt{\frac{\theta_A (1 - \theta_C w)}{\theta_A - \theta_C}} \frac{\pi}{2K(k)}, \ \langle a_{z\zeta} \rangle_e = 0,$$

$$\langle a_{z\xi}^2 \rangle_e = \frac{\theta_A (1 - \theta_C w)}{\theta_A - \theta_C} \frac{E(k)}{K(k)}, \ \langle a_{z\eta}^2 \rangle_e = \frac{1 - \theta_C w}{1 - \theta_C} \left(1 - \frac{E(k)}{K(k)} \right),$$

$$\langle a_{z\zeta}^2 \rangle_e = \frac{\theta_C (\theta_A w - 1)}{\theta_A - \theta_C} \left[1 - \frac{1}{k^2} \left(1 - \frac{E(k)}{K(k)} \right) \right]$$

where K(k) and E(k) are complete elliptic integrals of the first and second kind with modulus

$$k = \sqrt{\frac{(1 - \theta_C)(1 - \theta_A w)}{(1 - \theta_A)(1 - \theta_C w)}}$$

The value $\langle a_{z\xi} \rangle_e$ is positive for SAM₊ motions and negative for SAM₋ motions. If $1 < w \le \frac{1}{\theta_C}$ (LAM motion)

$$\langle a_{z\xi} \rangle_e = 0, \ \langle a_{z\zeta} \rangle_e = \pm \sqrt{\frac{\theta_C(\theta_A w - 1)}{\theta_A - \theta_C}} \frac{\pi}{2K(k)},$$

$$\langle a_{z\xi}^2 \rangle_e = \frac{\theta_A(1 - \theta_C w)}{\theta_A - \theta_C} \left[1 - \frac{1}{k^2} \left(1 - \frac{E(k)}{K(k)} \right) \right],$$

$$\langle a_{z\eta}^2 \rangle_e = \frac{1 - \theta_A w}{1 - \theta_A} \left(1 - \frac{E(k)}{K(k)} \right), \ \langle a_{z\zeta}^2 \rangle_e = \frac{\theta_C(\theta_A w - 1)}{\theta_A - \theta_C} \frac{E(k)}{K(k)},$$

$$k = \sqrt{\frac{(1 - \theta_A)(1 - \theta_C w)}{(1 - \theta_C)(1 - \theta_A w)}}.$$

The sign of $\langle a_{z\zeta} \rangle_e$ depends on whether the motion belongs to LAM+ or LAM_ .

The evolutionary equations for SAM and LAM have the same structure. To demonstrate this, one can rewrite Eqs. (6) in the following concise form:

$$\frac{d\mathbf{u}}{d\tau} = \begin{cases} \varepsilon \mathcal{F}_{\pm}(\theta_A, \theta_C, D_{0,1,2}^{\xi}, D_{1,2}^{\zeta}, \mathbf{u}), & \text{motion } \in SAM_{\pm} \quad \left(\frac{1}{\theta_A} \leq w < 1\right); \\ \varepsilon \mathcal{F}_{\pm}(\theta_C, \theta_A, D_{0,1,2}^{\zeta}, D_{1,2}^{\xi}, \mathbf{u}), & \text{motion } \in LAM_{\pm} \quad \left(1 < w \leq \frac{1}{\theta_C}\right). \end{cases}$$

Here $\mathbf{u} = (w, \rho, \sigma, L)^T$, \mathcal{F}_{\pm} is a certain vector-function depending on \mathbf{u} , the nucleus' inertia ellipsoid, and sublimation parameters.

Table II. Values of Φ_0 , Φ_1 for some comets

Comet	e	q	Φ_0	Φ_1
$2\mathrm{P/Encke}$	0.846	0.341	0.336	0.097
$46\mathrm{P/Wirtanen}$	0.652	1.063	0.068	0.039
$9P/Tempel\ 1$	0.519	1.500	0.040	0.027
19P/Borrelly	0.624	1.358	0.037	0.025
$1\mathrm{P/Halley}$	0.967	0.587	0.0084	0.0040
$_{ m 109P/Swift-Tuttle}$	0.9635	0.958	0.0026	0.0016

Note: The comets orbital parameters are according to [16]

Like the initial system (5), system (6) is reversible: if

$$(w(\tau), \rho(\tau), \sigma(\tau), L(\tau))^T$$

is a solution, then

$$(w(-\tau), \pi - \rho(-\tau), \pi + \sigma(-\tau), L(-\tau))^T$$

is also a solution of (6).

3.4. Parameters defining the behavior of solutions of the evolutionary equations

The parameters $D_0^{\xi,\zeta}$, $D_1^{\xi,\zeta}$, $D_2^{\xi,\zeta}$ in (6) are integral characteristics of the comet matter sublimation. If the nucleus is ellipsoidal and physical properties of its surface do not vary too strongly (the distributed mass ejection model), the values of these parameters satisfy

$$|D_0^{\xi,\zeta}| \sim |D_2^{\xi,\zeta}| \ll |D_1^{\xi,\zeta}|.$$

If mass ejection is localized over a small region of the surface,

$$|D_0^{\xi}| \ge |D_1^{\xi}|, \ |D_0^{\zeta}| \ge |D_1^{\zeta}|.$$

Parameters Φ_0 and Φ_1 are functions of the perihelion distance q and the eccentricity e. In Table II, values of Φ_0 and Φ_1 are presented for the comets listed in Table I. At large eccentricities ($e \approx 1$) one can use the approximate formulae

$$\Phi_0 pprox (1 - e^2)^{3/2} \Psi_0(q) \,, \,\, \Phi_1 pprox (1 - e^2)^{3/2} \Psi_1(q)$$

Table III. Values of Ψ_0 , Ψ_1 for some q

\overline{q}	Ψ_0	Ψ_1	Ψ_0 / Ψ_1
0.5	0.6975	0.3164	2.2047
0.6	0.4465	0.2221	2.0101
0.7	0.3028	0.1632	1.8558
0.8	0.2140	0.1236	1.7305
0.9	0.1556	0.0956	1.6269
1.0	0.1155	0.0750	1.5402
1.1	0.0870	0.0593	1.4670
1.2	0.0661	0.0471	1.4048
1.3	0.0505	0.0373	1.3516
1.4	0.0385	0.0295	1.3061
1.5	0.0293	0.0231	1.2672
1.6	0.0222	0.0180	1.2337
1.7	0.0166	0.0137	1.2051
1.8	0.0122	0.0103	1.1806
1.9	0.0089	0.0076	1.1597
2.0	0.0063	0.0055	1.1419

where

$$\Psi_0(q) = \frac{1}{\pi} \int_0^{\pi} g\left(\frac{2q}{1 + \cos \nu}\right) \frac{d\nu}{(1 + \cos \nu)^2}$$

$$\Psi_1(q) = \frac{1}{\pi} \int_0^{\pi} g\left(\frac{2q}{1 + \cos \nu}\right) \frac{\cos \nu d\nu}{(1 + \cos \nu)^2}$$

Values of functions $\Psi_0(q), \Psi_1(q)$ for several values of q are given in Table III. A more detailed analysis of the properties of these functions can be found in [19].

3.5. Probabilistic interpretation of changes in nucleus rotation mode

When $\varepsilon \neq 0$, changes in the mode of rotation can occur in the motions described by (5). At $w \approx 1$ one of the following transitions can take place, depending on initial conditions:

$$SAM_{\pm} \rightarrow SAM_{\mp}, \ LAM_{\pm} \rightarrow LAM_{\mp},$$
 $SAM \rightarrow LAM, \ LAM \rightarrow SAM.$

Fig.4. An example of change of mode at a separatrix crossing: $SAM_+ \rightarrow SAM_-$ (curve 1) and $SAM_+ \rightarrow LAM_+$ (curve 2). The initial conditions in the motions 1 and 2 differ only in the value of φ : $\varphi(0) = 120.0^{\circ}$ in the motion 1 and $\varphi(0) = 0.0^{\circ}$ in the motion 2. Values of the other parameters at $\tau = 0$ coincide in the both cases: $L(0) = 1.000, \rho(0) = 45.0^{\circ}, \sigma(0) = \psi(0) = 90.0^{\circ}$. Values of A, B, C, ε are equal to those given in **Sec. 2** and **Sec.3** for comet Halley. Orbital parameters are also the same as for comet Halley. Intensity distribution and position of active areas on the nucleus' surface correspond to the first Halley-like model nucleus discussed in **Sec. 5**.

A change in the mode of rotation implies that the phase trajectory of (5) crosses the separatrix which separates the different modes at $\varepsilon = 0$. In some cases even a small variation in initial conditions can affect the new mode's type (Fig. 4). Following [18], one can define the probabilities of various modes after separatrix crossing, but, unfortunately, methods for calculating these probabilities in multi-frequency systems have not been developed (in [18], only single-frequency systems were considered).

The evolutionary equations (6) in the limit $w \to 1$ can be used to describe the behavior of phase trajectories before and after a change in mode, but they cannot be used to study phenomena that occur during the separatrix crossing.

3.6. Conditions for the averaging approximation.

Application of the averaging approximation rests on the assumption that the variations in the rotational parameters over one orbit around the Sun are small enough. This is certainly valid if

$$\varepsilon_* = \varepsilon \Phi_0 \left(\frac{\Omega_*}{\Omega_0} \right) \ll 1,$$
(7)

where Ω_0 is the comet mean motion. The comets listed in Table I, do not meet condition (7): all of them have $\varepsilon_* \sim 1$. However, one should note that the parameter ε gives an excessive estimate of the effect of reactive torques on the nucleus rotation. Results of computer integrations show that even at $\varepsilon_* \sim 1$ the averaged equations give a good description of the nucleus' spin evolution, provided that the active zones are distributed realistically.

In addition, the averaging approximation assumes that capture into resonance does not take place. Rigorous results on the application of the averaging method in multi-frequency systems, presented in [1, 2], imply that generally equations (6) describe evolution of the nucleus rotation for the majority of initial conditions. The set of initial conditions where this is not true (whose measure tends to 0 as $\varepsilon \to 0$) consists mainly of those corresponding to solutions captured into a resonance. In this case a commensurability between frequencies of the perturbed Euler-Poinsot motion is preserved for a long time. To study solutions of (5) when a commensurability exists one can use the approach described in [2]. Taking into account the above mentioned "nongenerality" of resonant motions, we do not consider them in the present paper.

3.7. Evolutionary equations for nuclei with nearly axisymmetric inertia ellipsoids

In [19], the rotational evolution of a comet nucleus was studied under the assumption that its inertia ellipsoid was axially symmetric. In this subsection we show that the equations derived in [19] can be obtained as a limiting case of our current equations.

Here we only consider the case of a prolate nuclei:

$$\theta_A - 1 \ll 1 - \theta_C. \tag{8}$$

Use the parameter $\overline{\varepsilon} = \theta_A - 1$ to describe the proximity of the inertia ellipsoid to an axially symmetric one. If $w \in \left(1, \frac{1}{\theta_C}\right)$, $w-1 > c_0^{-1}$ (where c_0 is a positive constant that can be chosen arbitrarily large), then at sufficiently small values of $\overline{\varepsilon}$ the nutation angle oscillates with a small amplitude and the period T_{ϑ} around its mean value $\overline{\vartheta}$:

$$\vartheta = \overline{\vartheta} + O(\overline{\varepsilon}), \, \overline{\vartheta} = \begin{cases} \arccos \frac{\theta_A(w-1)}{1 - \theta_C} + O(\overline{\varepsilon}) & \text{for LAM}_+ \\ \pi - \arccos \frac{\theta_A(w-1)}{1 - \theta_C} + O(\overline{\varepsilon}) & \text{for LAM}_- \end{cases}$$
(9).

The condition $w-1>c_0^{-1}$ ensures that the polhode is far from the separatrices bounding the SAM \pm regions.

The angle $\overline{\vartheta}$ can be used instead of w as a parameter in the LAM family. Changing variables $w \to \overline{\vartheta}$, we rewrite (6) as follows:

$$\frac{d\overline{\vartheta}}{d\tau} = \frac{\varepsilon}{2L} [3\alpha \Phi_1 D_1^{\zeta} \cos \rho \cos \overline{\vartheta} - 2(1-\alpha)\Phi_0 D_0^{\zeta}] \sin \overline{\vartheta} + O(\varepsilon \overline{\varepsilon}), \qquad (10)$$

$$\begin{split} \frac{d\rho}{d\tau} &= -\frac{\varepsilon\alpha\sin\rho}{4L} D_1^{\zeta} \Phi_1(2 - 3\sin^2\overline{\vartheta}) + O(\varepsilon\overline{\varepsilon}) \,, \\ \frac{d\sigma}{d\tau} &= \frac{\varepsilon\alpha}{2L} D_2^{\zeta} \Phi_1\cos\overline{\vartheta} + O(\varepsilon\overline{\varepsilon}) \,, \\ \frac{dL}{d\tau} &= -\frac{\varepsilon}{2} \left[\alpha\Phi_1 D_1(2 - 3\sin^2\overline{\vartheta})\cos\rho - 2(1 - \alpha)\Phi_0 D_0\cos\overline{\vartheta} \right] + O(\varepsilon\overline{\varepsilon}) \,. \end{split}$$

Equations (10) at $\overline{\varepsilon} = 0$ coincide with the evolutionary equations in [19]. This implies that the conclusions about secular effects in nucleus motion made in [19] are also valid in the case when the inertia ellipsoid is slightly different from an axially symmetric one ($\overline{\varepsilon} \ll 1$).

Equations describing evolution of SAM cannot be simplified like this at $\overline{\varepsilon} \ll 1$. Even in the absence of perturbations ($\varepsilon = 0$), motions with $\vartheta \approx 90^{\circ}$ are essentially different at $\overline{\varepsilon} = 0$ and $\overline{\varepsilon} \neq 0$.

4. Quasi-stationary motions

An important property of (6) is the independence of its right hand side from the variable σ . This is due to symmetry of the moments applied to the nucleus before and after passage through the perihelion. Moreover, taking the independent variable as

$$\tau_* = \Phi_1 \int_0^\tau \frac{d\tau'}{L}$$

one obtains in (6) a closed subsystem for w and ρ :

$$\frac{dw}{d\tau_*} = 2\varepsilon \left\{ (1-\alpha)\Phi_0 \left[D_0^{\xi} \langle a_{z\xi} \rangle_e \left(\frac{1}{\theta_A} - w \right) + D_0^{\zeta} \langle a_{z\zeta} \rangle_e \left(\frac{1}{\theta_C} - w \right) \right] - (11) \right. \\
\left. - \alpha \cos \rho \Phi_1 \left[D_1^{\xi} \left(\left(\frac{1}{\theta_A} - w \right) \langle a_{z\xi}^2 \rangle_e - (1-w) \langle a_{z\eta}^2 \rangle_e \right) + \right. \\
\left. + D_1^{\zeta} \left(\left(\frac{1}{\theta_C} - w \right) \langle a_{z\zeta}^2 \rangle_e - (1-w) \langle a_{z\eta}^2 \rangle_e \right) \right] \right\}, \\
\frac{d\rho}{d\tau_*} = -\frac{\varepsilon \alpha \sin \rho \Phi_1}{2} \left[D_1^{\xi} (\langle a_{z\xi}^2 \rangle_e - \langle a_{z\eta}^2 \rangle_e) + D_1^{\zeta} (\langle a_{z\zeta}^2 \rangle_e - \langle a_{z\eta}^2 \rangle_e) \right].$$

If (w^*, ρ^*) is a stationary solution of (11), then (6) admits the quasistationary solution

$$\mathbf{u}^* = (w^*, \rho^*, \sigma^*(\tau), L^*(\tau))^T,$$

$$\sigma^*(\tau) = \varepsilon c_\sigma \int_0^\tau \frac{d\tau'}{L^*(\tau')} + \sigma_o^*, \ L^*(\tau) = \varepsilon c_L \tau + L_o^*,$$

$$(12)$$

where the constants c_{σ} and c_{L} can be easily found after substituting w^{*} , ρ^{*} into the corresponding equations of (6). The constants σ_{\circ}^{*} , L_{\circ}^{*} are the initial values of the angle σ and the dimensionless angular momentum in the quasi-stationary motion under consideration.

The quasi-stationary motions defined in Eq. (12) can be divided into three classes.

Class A: trivial quasi-stationary motions. For all values of the parameters $D_0^{\xi,\zeta}, D_1^{\xi,\zeta}, \Phi_{0,1}$ there exist degenerate quasi-stationary motions with the angular momentum vector directed along the OZ axis $(\sin \rho^* = 0)$ and a simple SAM $(w^* = \frac{1}{\theta_A})$ or simple LAM $(w^* = \frac{1}{\theta_C})$ rotation mode. If

$$|\kappa_{m{\xi}}| > \kappa_0, \; \kappa_{m{\xi}} = rac{\Phi_0 D_0^{m{\xi}}}{\Phi_1 D_1^{m{\xi}}}, \; \kappa_0 = rac{3lpha}{2(1-lpha)},$$

there are simple SAM motions of Class A that are stable with respect to variables w^*, ρ^* . If

$$|\kappa_\zeta| > \kappa_0, \; \kappa_\zeta = rac{\Phi_0 D_0^\zeta}{\Phi_1 D_1^\zeta}$$

Table IV. Stability conditions for motions of the class A

	Motion		Stability conditions		
$ ho^* = 0 \; (\mathbf{L} \uparrow \uparrow \mathbf{r}_{\pi})$	$w_* = rac{1}{ heta_A}$	simple SAM ₊	$D_1^{\xi} > 0, \ \kappa_{\xi} > \kappa_0$		
		$\begin{array}{ll} \text{simple SAM}_{+} & D_{1}^{\xi} > 0, \ \kappa_{\xi} > \kappa_{0} \\ \\ \text{simple SAM}_{-} & D_{1}^{\xi} > 0, \ \kappa_{\xi} < -\kappa_{0} \\ \\ \text{simple LAM}_{+} & D_{1}^{\zeta} > 0, \ \kappa_{\zeta} > \kappa_{0} \\ \\ \text{simple LAM}_{-} & D_{1}^{\zeta} > 0, \ \kappa_{\zeta} < -\kappa_{0} \\ \\ \text{simple SAM}_{+} & D_{1}^{\xi} < 0, \ \kappa_{\xi} < -\kappa_{0} \\ \\ \\ \text{simple SAM}_{-} & D_{1}^{\xi} < 0, \ \kappa_{\xi} > \kappa_{0} \end{array}$			
	$w_* = rac{1}{ heta_C}$.	simple LAM_+	$D_1^{\zeta}>0,\;\kappa_{\zeta}>\kappa_0$		
	$w_* - \theta_C$	$\mathrm{simple} \ \mathrm{LAM}_{-}$	$D_{1}^{\xi} > 0, \ \kappa_{\xi} < -\kappa_{0}$ $D_{1}^{\zeta} > 0, \ \kappa_{\zeta} > \kappa_{0}$ $D_{1}^{\zeta} > 0, \ \kappa_{\zeta} < -\kappa_{0}$ $D_{1}^{\xi} > 0, \ \kappa_{\xi} < -\kappa_{0}$ $D_{1}^{\xi} < 0, \ \kappa_{\xi} < -\kappa_{0}$ $D_{1}^{\xi} < 0, \ \kappa_{\xi} > \kappa_{0}$ $D_{1}^{\zeta} < 0, \ \kappa_{\zeta} < -\kappa_{0}$		
$ ho^* = \pi \; (\mathbf{L} \uparrow \downarrow \mathbf{r}_\pi)$	w _ <u>1</u>	$\mathrm{simple}\;\mathrm{SAM}_{+}$	<u> </u>		
	$w_* = rac{1}{ heta_A}$				
	$w_* = rac{1}{ heta_C}$	simple LAM_+	$D_1^{\zeta} < 0, \; \kappa_{\zeta} < -\kappa_0$		
	$w_* - \overline{\theta_C}$	$\mathrm{simple} \mathrm{LAM}_{-}$	$D_1^{\zeta} < 0, \; \kappa_{\zeta} > \kappa_0$		

there are simple LAM motions that are stable in the same sense. More detailed information on the stable motions of Class A are given in Table IV.

Class B: The angular momentum vector is parallel to the radius vector of the comet at the perihelion ($\mathbf{L} \uparrow \uparrow \mathbf{r}_{\pi}$ or $\mathbf{L} \uparrow \downarrow \mathbf{r}_{\pi}$). The point where the straight line containing the nucleus' angular velocity vector crosses its inertia ellipsoid moves faster and faster ($c_L > 0$) or slower and slower ($c_L < 0$) along the polhode corresponding to the unperturbed motion at $w = w^*$ (SAM at $w^* < 1$ and LAM at $w^* > 1$).

Quasi-stationary complex SAMs of Class B exist if

$$\kappa_{\xi}^* < |\kappa_{\xi}| < \kappa_{\xi}^{**},\tag{13}$$

where

$$\kappa_{\xi}^{*} = \inf_{w \in (\frac{1}{\theta_{A}}, 1)} \frac{\alpha |G_{\xi}(w) + \chi G_{\zeta}(w)|}{(1 - \alpha) F_{\xi}(w)}, \quad \kappa_{\xi}^{**} = \sup_{w \in (\frac{1}{\theta_{A}}, 1)} \frac{\alpha |G_{\xi}(w) + \chi G_{\zeta}(w)|}{(1 - \alpha) F_{\xi}(w)},$$

$$G_{\xi}(w) = \left(\frac{1}{\theta_{A}} - w\right) \langle a_{z\xi}^{2} \rangle_{e} - (1 - w) \langle a_{z\eta}^{2} \rangle_{e},$$

$$G_{\zeta}(w) = \left(\frac{1}{\theta_{C}} - w\right) \langle a_{z\zeta}^{2} \rangle_{e} - (1 - w) \langle a_{z\eta}^{2} \rangle_{e},$$

$$F_{\xi}(w) = |\langle a_{z\xi} \rangle_{e}| \left(w - \frac{1}{\theta_{A}}\right), \quad \chi = \frac{D_{1}^{\zeta}}{D_{1}^{\xi}}.$$

Condition (13) ensures that at $\sin \rho^* = 0$ and $w = w^* \in \left(\frac{1}{\theta_A}, 1\right)$ the right hand side of the first equation in (11) is zero.

One can similarly write the condition for existence of complex LAMs of Class B:

$$\kappa_{\zeta}^{*} < |\kappa_{\zeta}| < \kappa_{\zeta}^{**}, \tag{14}$$

where

$$\kappa_{\zeta}^* = \inf_{w \in (1, \frac{1}{\theta_C})} \frac{\alpha \left| \frac{G_{\xi}(w)}{\chi} + G_{\zeta}(w) \right|}{(1 - \alpha)F_{\zeta}(w)}, \ \kappa_{\zeta}^{**} = \sup_{w \in (1, \frac{1}{\theta_C})} \frac{\alpha \left| \frac{G_{\xi}(w)}{\chi} + G_{\zeta}(w) \right|}{(1 - \alpha)F_{\zeta}(w)},$$

$$F_{\zeta}(w) = |\langle a_{z\zeta}
angle_e| \left(rac{1}{ heta_C} - w
ight).$$

Class C: The nucleus' angular momentum vector \mathbf{L} precesses at a constant angle ρ^* around the OZ axis, which is parallel to the comet's radius vector at the perihelion. The nucleus' motion with respect to the angular momentum vector (SAM at $w^* < 1$ and LAM at $w^* > 1$) is exactly the same as in motions of Class B.

The value of w^* in Class C motions should satisfy the condition

$$\frac{H_{\xi}(w^*)}{H_{\zeta}(w^*)} = -\chi,\tag{15}$$

where

$$H_{\xi}(w) = \langle a_{z\xi}^2 \rangle_e - \langle a_{z\eta}^2 \rangle_e, \ H_{\zeta}(w) = \langle a_{z\zeta}^2 \rangle_e - \langle a_{z\eta}^2 \rangle_e.$$

Assume it is possible to select w^* to satisfy condition (15) at a certain value of χ . If $w^* \in \left(\frac{1}{\theta_A}, 1\right)$, then a quasi-stationary motion of Class C exists provided that

$$|\kappa_{\xi}| < rac{lpha |G_{\xi}(w^*) + \chi G_{\zeta}(w^*)|}{(1-lpha)F_{\xi}(w^*)}.$$

If $w^* \in (1, \frac{1}{\theta_C})$, then the condition of existence of Class C motion takes the form:

$$|\kappa_\zeta| < rac{lpha|rac{G_\xi(w^*)}{\chi} + G_\zeta(w^*)|}{(1-lpha)F_{\mathcal{L}}(w^*)}.$$

It follows that the types of quasi-stationary motions that can exist for a nucleus with a certain given distribution of active zones depend on the values of parameters χ , κ_{ξ} , κ_{ζ} (properties of quasi-stationary SAMs depend on χ , κ_{ξ} ; properties of LAMs depend on χ , κ_{ζ}).

In Fig. 5 we present the separation of the set of values of these parameters into areas with different combinations of possible quasi-stationary motions for a nucleus with moment of inertia ratios equal to those for comet Halley (Sec. 2).

Fig.5. Classification of quasi-stationary SAMs (left) and LAMs (right), existing at corresponding values of parameters κ_{ξ} , κ_{ζ} , χ . The values of these parameters for the first and second variants of active zones relative intensities for model Halley nucleus (Sec.5) are marked with the symbols \star and \circ correspondingly.

The type of quasi-stationary motions is important for classification. It can be used to distinguish nuclei with different scenarios of rotational evolution. We suppose that a more detailed description of the diversity of such scenarios would be a formal exercise, due to very rough correspondence between the empirical mass ejection model and the real processes. Therefore, we restrict ourselves to consider several examples based on spacecraft observations of the nuclei of comets Halley and Borrelly.

5. Evolutionary paths for a Halley-like nucleus

It was shown in [4] that, based on the images of the comet Halley nucleus transmitted by the "Vega 1,2" and "Giotto" spacecraft, one can conclude that there are five active zones. We consider the dynamics of rotation for various intensities of mass ejection at these zones.

Suppose that the centers of the active zones are the points on the nucleus surface presented in Table V. Within the accuracy to which the active zones can be identified, this assumption agrees with the results in [4]. The nucleus of comet Halley is essentially non-convex (see Fig. 1). However, for this distribution of active zones one can neglect effects due to the shadowing of the zones with other parts of the nucleus. Indeed, based on ideas of [8], we take the following parameter to describe shadowing of the j-th face:

$$\delta_j^* = \min_{\mathbf{e} \in \mathcal{E}_j} \left[\arccos(\mathbf{n}_j, \mathbf{e}) \right],$$

where \mathcal{E}_j is a set of unit vectors defining directions from the center of this face to points of the nucleus' surface belonging to the edges of the approximating polyhedron. If the angle δ_j between the outer normal \mathbf{n}_j and the direction to the Sun is smaller than δ_j^* , the centre of the face is lighted at any orientation of the nucleus satisfying this condition. In particular, in the case $\delta_j^* = 90^\circ$ the face belongs to the convex part of the nucleus' surface (or, more rigorously, to the convex hull of the approximating polyhedron), and it cannot be shadowed for $\delta_j < 90^\circ$.

According to our calculations, for Halley nucleus model in use and accepted positions of active zones we have

$$\delta_1^* = \delta_2^* = \delta_5^* = 90^\circ, \ \delta_3^* = 86^\circ, \ \delta_4^* = 87^\circ.$$

Table V. Position and orientation of the active zones for Halley-like model nucleus

Zone 1	$egin{array}{c} \mathbf{R}_1 \\ \mathbf{n}_1 \end{array}$	$R_*(-0.22059, 0.28199, -1.44677)_{O\xi\eta\zeta}^T \ (-0.32714, 0.85784, -0.39936)_{O\xi\eta\zeta}^T$
Zone 2	$egin{array}{c} \mathbf{R}_2 \ \mathbf{n}_2 \end{array}$	$R_*(0.19626, 0.39703, 0.97325)_{O\xi\eta\zeta}^T$ $(0.04046, 0.61546, 0.78713)_{O\xi\eta\zeta}^T$
Zone 3	$egin{array}{c} \mathbf{R}_3 \ \mathbf{n}_3 \end{array}$	$R_*(-0.46986, -0.43157, 0.99487)_{O\xi\eta\zeta}^T (-0.87622, -0.41999, 0.23632)_{O\xi\eta\zeta}^T$
Zone 4	$egin{array}{c} \mathbf{R}_4 \\ \mathbf{n}_4 \end{array}$	$R_*(0.17474, 0.77468, -0.26201)_{O\xi\eta\zeta}^T $ $(0.15729, 0.93500, -0.31786)_{O\xi\eta\zeta}^T$
Zone 5	$egin{array}{c} \mathbf{R}_5 \ \mathbf{n}_5 \end{array}$	$R_*(0.31496, -0.61161, -0.72302)_{O\xi\eta\zeta}^T \ (0.24348, -0.96664, -0.07947)_{O\xi\eta\zeta}^T$

Table VI. Dynamic parameters of Halley-like model nucleus

Description		Variant 1	Variant 2
Integral mass ejection parameters	D_0^{ξ} D_1^{ξ} D_2^{ξ}	-0.30703 0.17284 -0.09872	-0.21455 0.15312 -0.12508
	$D_0^{\zeta} \\ D_1^{\zeta} \\ D_2^{\zeta}$	$0.04422 \\ -0.01420 \\ 0.32992$	-0.00365 -0.05161 0.27154
Classification parameters	$\kappa_{\xi} \ \kappa_{\zeta} \ \chi$	-3.69341 -6.47612 -0.08214	$-2.91326 \\ 0.14723 \\ -0.33704$

Therefore, only active zones 3 and 4 can be shadowed. However, the range of angles where (4) cannot be applied due to the shadowing effects is quite small (less than 4°). Hence, the difference between the averaged equations obtained with the use of (4) and its hypothetical modification taking shadowing effects into account is insignificant. Moreover, this difference is absolutely unimportant because of very approximate correspondence of the accepted matter sublimation model and the real processes.

We consider two possible cases for the zone activity levels (values of the integral parameters of mass ejection are shown in Table VI). The first case is the most probable for the nucleus of comet Halley and was suggested in [4]:

$$s_1 = s_4 = \frac{1}{3}, \ s_2 = s_3 = s_5 = \frac{1}{9}.$$

The phase portrait of system (11) showing secular evolution of variables w and ρ at such a distribution of the intensities is shown in Fig. 6. One can see that the stable quasi-stationary modes are motions of Class A: simple LAM₊, $\mathbf{L} \uparrow \downarrow \mathbf{r}_{\pi}$ and simple SAM₋, $\mathbf{L} \uparrow \uparrow \mathbf{r}_{\pi}$. The shading denotes a decreasing angular momentum (spin-down). If a phase point $(w(\tau), \rho(\tau))$ is in the non-shaded part of the phase portrait, the nucleus spins up.

The second case corresponds to mass ejection primarily from active zones 1 and 2:

$$s_1 = \frac{1}{3}, \ s_2 = \frac{1}{2}, \ s_3 = s_4 = s_5 = \frac{1}{18}.$$

The phase portrait of system (11) for such a nucleus is shown in Fig. 7. Together with a stable quasi-stationary motion of Class A (simple SAM₋, $\mathbf{L} \uparrow \uparrow \mathbf{r}_{\pi}$) there also exists a stable quasi-stationary motion of Class C, that is complex LAM₋ ($w^* \approx 1.532$). In this latter motion, the angle between angular momentum vector \mathbf{L} and vector \mathbf{r}_{π} is $\approx 99.8^{\circ}$. Note, that at $w^* \approx 1.532$ the angle ϑ between \mathbf{L} and the axis $O\zeta$ of the body-fixed coordinate system varies from $\approx 55.5^{\circ}$ to $\approx 56.5^{\circ}$.

These examples demonstrate that evolution depends not only on the location of active zones, but on their respective intensities as well.

Fig.6. Phase trajectories of (11) at the distribution of intensities of the active zones according to [4]

Fig.7. Phase trajectories of (11) for Halley-like nucleus with principal mass ejection in the active zones 1 and 2

6. Dynamic properties of a Borrelly-like nucleus

Detailed images of the nucleus of comet 19P/Borrelly were obtained by the "Deep Space-1" mission [12]. Approximate reconstruction of the nucleus' shape based on these images and observations by Hubble Space Telescope [14] is shown in Fig. 8. The nucleus can be approximated as a combination of two ellipsoids with major semi-axes 1.6 km, 1.8 km, 3.0 km and 0.96 km, 1.08 km, 1.8 km accordingly. The distance between the centers of these ellipsoids is 3.7 km. Assuming that the nucleus is homogeneous, one obtains:

$$\theta_A = 1.03038, \ \theta_C = 0.25886.$$

The images indicate the existence of three active zones in the middle region of the nucleus. Assume for definiteness that in the body-fixed reference frame $O\xi\eta\zeta$ the centers of these active zones are defined by radius-vectors $\mathbf{R}_1, \mathbf{R}_2, \mathbf{R}_3$ presented in Table VII. The parameters of mass ejection calculated for the case of equal intensities of the zones have the following values:

$$\begin{split} D_0^\xi &= 0.00211, \ D_1^\xi = 0.00202, \ D_2^\xi = 0.01394, \\ D_0^\zeta &= -0.00218, \ D_1^\zeta = -0.00043, \ D_2^\zeta = -0.04985. \end{split}$$

The main qualitative properties of secular evolution for the nucleus rotation are determined by parameters κ_{ξ} , κ_{ζ} , χ . In the case considered

$$\kappa_{\xi} = 1.55418, \ \kappa_{\zeta} = 7.59512, \ \chi = -0.21128.$$

With the use of expressions obtained in Section 4, one can find that this nucleus can perform a stable, quasi-stationary motion of Class A, that is simple SAM with the angular momentum vector directed along the line of apsides. Such a mode of rotation is supposed to be the most probable one for the real P/Borrelly nucleus.

Table VII. Position and orientation of the active zones for Borrelly-like model nucleus

Zone 1	\mathbf{R}_1	$R_*(-0.36292, 0.10853, -0.40400)_{O\xi\eta\zeta}^T$
	\mathbf{n}_1	$(0.95555, 0.23511, 0.17789)_{O\xi\eta\zeta}^T$
Zone 2	${f R}_2$	$R_*(0.35606, 0.01017, -0.31896)_{O\xi\eta\zeta}^T$
	\mathbf{n}_2	$(0.96787, 0.03299, 0.24927)_{O\xi\eta\zeta}^T$
Zone 3	${f R}_3$	$R_*(0.36711, -0.08721, -0.40252)_{O\xi\eta\zeta}^T$
2010 0	\mathbf{n}_3	$(0.96978, -0.16768, 0.17722)_{O\xi\eta\zeta}^{T}$

Fig.8. P/Borrelly nucleus: rough reconstruction based on Deep Space-1 images

Conclusions

Using the averaging method, we obtained evolutionary equations describing the secular effect of outgassing on the rotation of comet nuclei. We indicated parameters that determine qualitative properties of evolution of nucleus rotation. Classification of possible quasi-stationary modes of motion was also given.

Acknowledgements

This work was supported by the NASA JURRISS program under Grant NAG5-8715. AIN, AAV, and VVS acknowledge support from Russian Foundation for Basic Researches via Grants 00-01-00538 and 00-00-00174 respectively. Also they acknowledge support from INTAS via Grant 00-221. DJS acknowledges support from the PG&G program via Grant NAG5-9017.

References

- [1] Arnold, V.I.: Mathematical Methods of Classical Mechanics. Springer, New York, 1978.
- [2] Arnold, V.I., V.V.Kozlov, and A.I.Neishtadt: Mathematical Aspects of Classical and Celestial Mechanics (Encyclopaedia of Mathematical Sciences, 3). Springer, Berlin, 1988.
- [3] Beletskii, V.I.: Motion of an Artificial Satellite about its Center of Mass. Israel program for scientific translations, Jerusalem, 1966.
- [4] Belton, M.J.S., W.H.Julian, A.J.Anderson, and B.E.A.Mueller: 1991 'The spin state and homogeneity of comet Halley's nucleus', *Icarus*, **93**, 183–193.
- [5] N.N.Bogolyubov and Yu.A.Mitropolsky: Asymptotic Methods in the Theory of Nonlinear Oscillations. Gordon and Breach Science Publ., New York, 1961.
- [6] Crifo, J.F. and A.V.Rodionov: 1999, 'Modelling the circumnuclear coma of comets: objectives, methods and recent results', *Planetary and Space Science*, 47, 797–826.
- [7] Dobrovolskis, A.R.: 1996, 'Inertia of any polyhedron', *Icarus*, 124, 698–704.
- [8] Gutierrez, P.G., J.L.Ortiz, R.Rodrigo, and J.J.López-Moreno: 2000, 'A study of water production and temperatures of rotating irregularly shaped cometary nuclei', Astron. Astrophys., 355, 809–817.
- [9] Jorda, L. and J.Licandro: (in press), 'Modeling the rotation of comets', Proceedings of the IAU Colloquim 168, held in Nanjing, China. Pub. Astron. Soc. Pacific.
- [10] Julian, W.H.: 1990, 'The comet Halley nucleus: random jets', *Icarus*, 88, 355–371.
- [11] Kamél, L.: 1991, 'The evolution of P/Encke's light curve: no secular fading, a vanishing perihelion asymmetry', *Icarus*, **93**, 226–245.
- [12] Kerr, R.A.: 2001, 'Close look at the heart of Borrelly', Science, 294, 27–28.

- [13] Kinoshita, H.: 1992, 'Analytical expansions of torque-free motions for short and long axis modes', Celes. Mech., 53, 365-375.
- [14] Lamy, P.L., I.Toth, and H.A.Weaver: 1998, 'Hubble Space Telescope observations of the nucleus and inner coma of comet 19P/1904 Y2 (Borrelly)', Astron. Astrophys., 337, 945-954.
- [15] Landau, L.D. and E.M.Lifshitz: *Mechanics*. Pergamon Press, Oxford, 1976.
- [16] Marsden, B.G. and G.V.Williams: Catalogue of Cometary Orbits. Smithsonian Astrophys. Obs., Cambridge. 1996.
- [17] Marsden, B.G., Z.Sekanina, and D.K.Yeomans: 1973, 'Comets and nongravitational forces.V', Astron. J., 78, 211–225.
- [18] Neishtadt, A.I.: 1991, 'Probability phenomena due to separatrix crossing', Chaos, 1, 42-48.
- [19] Neishtadt, A.I., D.J.Scheeres, V.V.Sidorenko, and A.A.Vasiliev: 2002, 'Evolution of comet nucleus rotation', *Icarus* (accepted for publication).
- [20] Peale, S.J. and J.J.Lissauer: 1989, 'Rotation of Halley's comet' *Icarus*, 79, 396–430.
- [21] Samarasinha, N.H. and M.J.S.Belton: 1995, 'Long-term evolution of rotational states and nongravitational effects for Halley-like cometary nuclei', *Icarus*, 116, 340–358.
- [22] Stooke, P.J. and A.Abergel: 1991, 'Morphology of the nucleus of comet P/Halley', Astron. Astrophys., 248, 656-668.
- [23] Stooke, P.J. and A.Abergel: 'Numeric shape model P/Halley nucleus' (unpublished)
- [24] Szegö, K., J.F.Crifo, L.Földy, J.S.V.Lagerros, and A.V.Rodionov: 2001, 'Dynamical effects of comet P/Halley gas production', Astron. Astrophys., 370, L35–L38.
- [25] Weeks, C.J.: 1995, 'The effect of comet outgassing and dust emission on the navigation of an orbiting spacecraft', J. Astronaut. Sci., 43, 327-343.
- [26] Whipple, F.L.: 1951, 'A comet model.I. Acceleration of comet Encke' Astrophys. J., 113, 464-474.
- [27] Wilhelm, K.: 1987, 'Rotation and precession of comet Halley', *Nature*, 327, 27–30.